

Behaviour of preproduction VPTs for the CMS Endcap Electromagnetic Calorimeter

20 April 2001

K.W.Bell, R.M.Brown, D.J.A.Cockerill, B.W.Kennedy, A.L.Lintern,
M.Sproston, A.M.Turner, J.H.Williams

Rutherford Appleton Laboratory, Chilton, Didcot, Oxfordshire, GB

P.R.Hobson, D.C.Imrie, C.Selby, O.Sharif

Brunel University, Uxbridge, Middlesex, GB

Abstract

This note reports measurements made on a preproduction batch of 500 Vacuum PhotoTriodes (VPTs) manufactured by RIE (St Petersburg) for the CMS Electromagnetic Endcap Calorimeter.

Introduction

This document describes a series of measurements made on a preproduction batch of 500 Vacuum PhotoTriodes (VPTs) manufactured by RIE (St Petersburg) for the CMS Electromagnetic Endcap Calorimeter. The VPTs were delivered in two batches; an initial delivery of 100 received in September 2000 (Batch I), and the remaining 400 delivered in December 2000 (Batch II). The two batches show some slight differences; where relevant, they are described separately in this report.

The appraisal of the VPTs was carried out at Brunel University and at RAL during the period September 2000-April 2001.

The VPT specification

Some of the technical specifications of the VPTs which are incorporated into the contractual agreement with the manufacturers are summarised in Table 1. A more detailed and definitive statement of the requirements can be found in [1].

Quantity	Meaning	Range
P	Photocathode quantum efficiency at 420nm	$\geq 18\%$
G	Current gain at zero field	≥ 8
B	Burn-in ratio	≥ 0.8
R	(Response at 4T)/(Response at 0T)	≥ 0.75
Q	$Q = P \times G \times B \times R$	≥ 1.15
F	Excess noise factor	< 4.0
i_{\max}^a	Maximum anode current from 0 - 4T	≤ 2 nA
Length	Overall length of VPT	≤ 46 mm
Stub length	Length of seal-off stub	≤ 14 mm
Diameter	External diameter of insulating sleeve	26.3-26.5mm

Table 1. Technical specification of VPTs. Measurements are to be made with anode and dynode voltages of 1000V and 800V respectively relative to the photocathode, using a blue LED of 430nm wavelength.

The RAL variable-angle test rig

Overview

The test rig at RAL is based on a conventional magnet providing fields up to 1.8T over an area of approximately 0.5 m². The vertical distance between the pole tips is approximately 10cm. VPTs are held in rows of 8 aluminium cans. Up to 6 such rows can be mounted in the rig, and each row of 8 cans may be rotated to present the VPTs to the magnetic field at any desired angle up to 90°.

Mechanical design

Figure 1 is a photograph of the RAL test rig area. The 1.8T magnet, slightly to the left of centre in the picture, was formerly used as a bending magnet in a beam line. The pole pieces are 50cm×90cm in area, with a gap of 10cm. The uniform field region is large enough to accommodate up to 48 VPTs simultaneously.

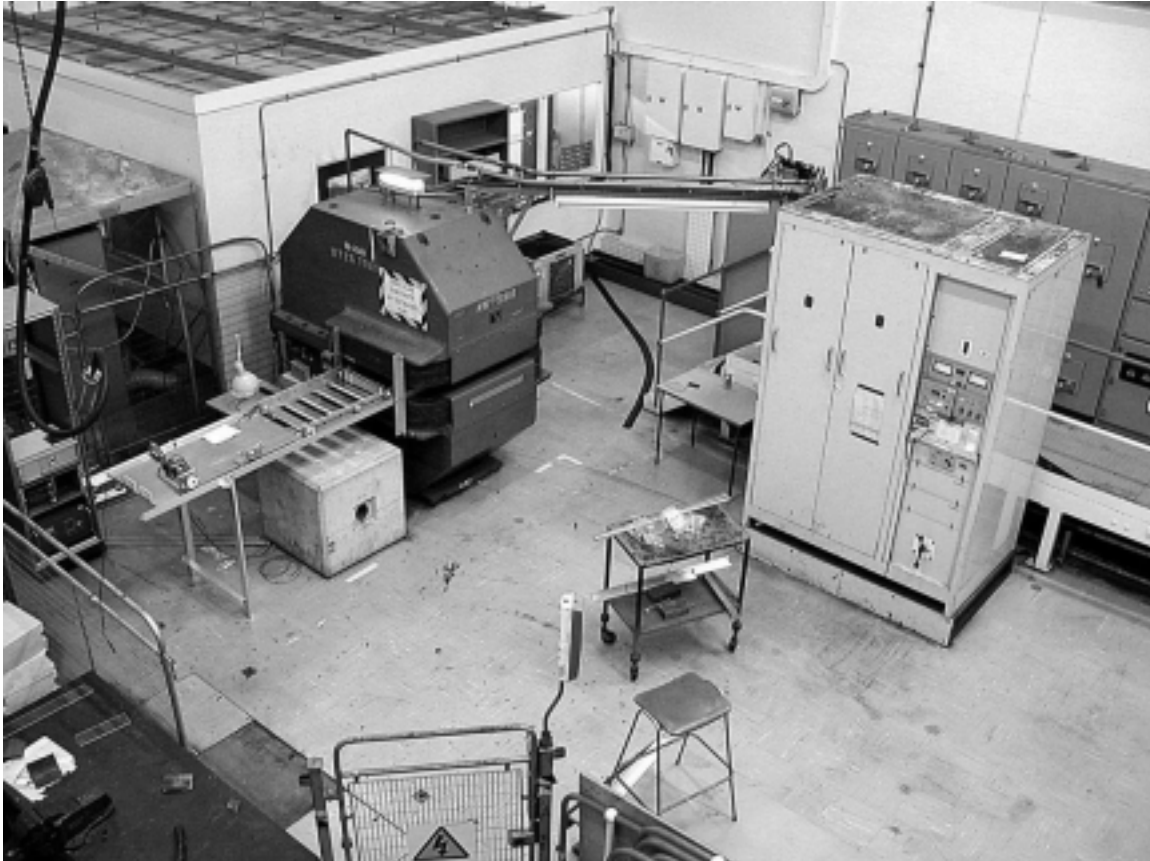


Figure 1. General view of the RAL test rig

The VPTs are held in aluminium cans; Figure 2 shows an example. Cans are glued together in rows of eight, with each row attached to the rig by a shaft, so that it may be rotated to present the VPTs at any desired angle to the magnetic field. A stepper motor is used to rotate all of the VPTs simultaneously by means of a system of drive belts.

When the rig is in use, the magnet pole tips are covered with a black cloth to eliminate stray light.

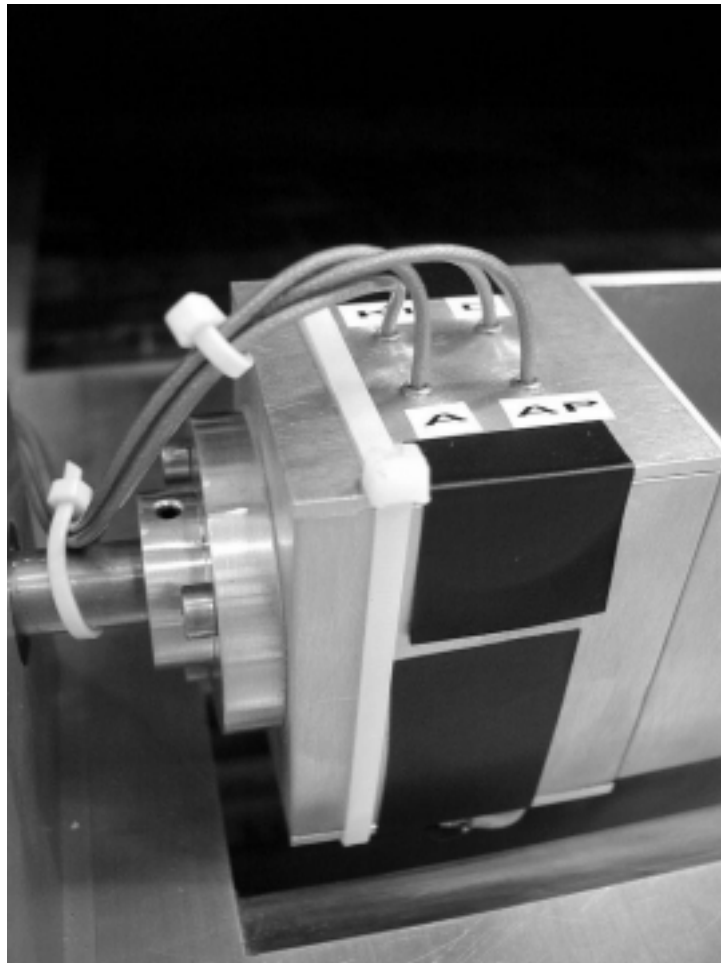


Figure 2. Close-up view of a VPT holder.

Illumination of photocathodes

Considerable care has been taken to illuminate the photocathodes as uniformly as possible. Each VPT is illuminated by a diffuser plate equipped with four 430nm LEDs, as illustrated in Figure 3. A metal mask is used to block the direct light from the LEDs, and to reduce electronic pick-up from the LED drive pulse.

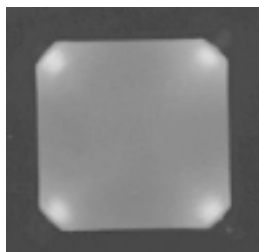


Figure 3. Frosted perspex diffuser plate equipped with four 430nm blue LEDs. In operation, the direct light from the LEDs is masked.

Electronics

Figure 4 shows a schematic diagram of the control and readout logic of the RAL test system. The system is constructed from standard CAMAC and NIM modules, with the exception of the anode signal amplifiers, which are low-noise devices designed at RAL. The HT power supply for the VPTs is an ISEG NHQ 222M high-precision unit allowing the output current to be monitored with a precision of 100pA.

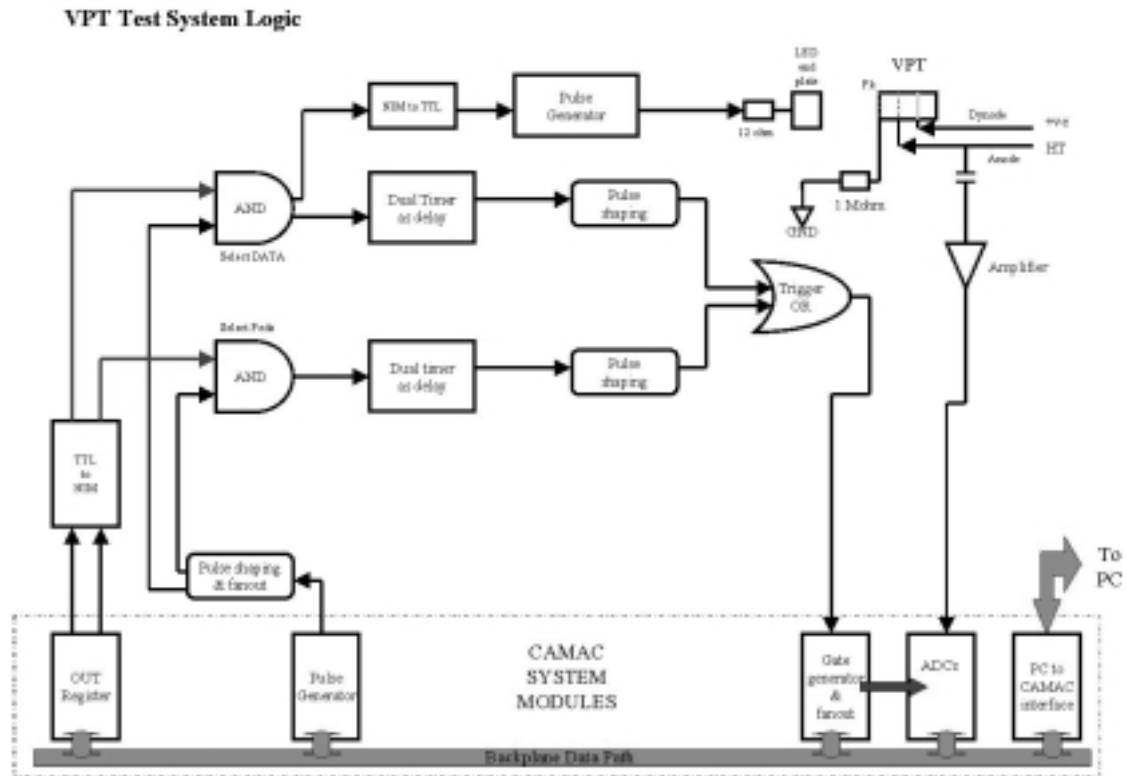


Figure 4. Schematic diagram of the VPT test system electronics

The DAQ and control software

The HT control and data acquisition systems are controlled by a PC running LabView software written at RAL. The 1.8T magnet is controlled by a Visual Basic program running on the same PC.

A second PC runs a simple database system to allow the bar codes to be automatically registered when VPTs are loaded into the test rig. For safety reasons, this PC also controls a small 'web-cam' which views the test rig area; images from this camera may be viewed remotely by means of a web-browser.

The Brunel high-field test system

Overview

The VPT test system at Brunel is specifically designed to measure the performance of tubes at the full CMS field of 4.0T. The tubes are measured at a single, fixed, angle of 15°. The small magnetised volume constrains the system to measuring only one tube at a time. The system is controlled by a number of IEEE488.2 devices using LabView software. The data acquisition is based around two IEEE488.2 Digital Multimeters (DMMs) and a multiplexed ADC card which resides in a PCI slot of a Pentium-II based PC.

Mechanical design

The 4T superconducting magnet is of the persistent current, through-bore solenoid, type and was originally part of an NMR spectrometer. The magnetised volume is very uniform but only 55 mm in diameter by approximately 100 mm in axial length. This constrains the mechanical design of the VPT holder to be a long cylindrical tube (known as a torpedo) in which up to six tubes will eventually be placed along the cylinder axis. The current version, used for all the preproduction tests, only holds a single tube at a fixed angle to the field of 15°.

Electronics

The overall schematic of the control and data acquisition system is shown in Figure 5. A PC, running LabView, is used to control the anode and dynode HT supplies, the two DMM reading anode and dynode currents plus monitoring of a number of voltage supplies. The same PC contains a 32 channel differential input 16-bit multiplexed ADC card which is used to acquire the pulsed LED response of the tubes under test. The step-motor system, which will be used to locate each one of the six VPT under test in the full-field region of the magnet, is controlled via an RS232 port. This part of the system is yet to be implemented.

Inside the torpedo the VPT anode is connected, via a high-voltage blocking capacitor, to a low-noise pre-amplifier. In the current single VPT torpedo, a blue LED, placed in a low-field region of approximately 0.1T, provides a light pulse to the VPT via a 1.0 mm diameter optical fibre.

The DAQ and control software

The 4T test system is controlled using specially developed LabView based software. A number of devices (HT supplies and voltage and current monitoring) are controlled via an IEEE488.2 bus. The anode currents of the VPT are calculated from measuring the small voltage drop across a 1M Ω nominal resistor. Both ends of this resistor are at the full anode HT (1000 V nominal) which exceeds the common mode rating of commercial DMM. To avoid having to develop and maintain special hardware we connected the last DMM to the IEEE488.2 bus via an opto-isolated bus extender. This allows the final branch of the bus to be up to 1.5 kV above ground. The isolated DMM is connected to the main AC supply via a 1:1 isolation transformer, and the AC ground of the DVM is

connected via a safety resistor to the anode HT, thus floating the whole DMM up to anode potential.

The cathode current, again measured using the voltage drop across a $1\text{M}\Omega$ resistor, and other voltages (for example the \pm preamplifier supplies) are connected to the second, non-isolated, DMM.

A dedicated pulse system, using a fast discharge of a capacitor connected to a precise DC voltage, drives the LED at one-half of the ADC trigger rate of 1kHz. This enables us to acquire alternate pedestal and signal information during the 10s DAQ period. A number of 10s pre-trigger cycles are executed to ensure thermal stability of the LED during the final DAQ cycle. The pulse height from the VPT is measured using a 16-bit 32-channel differential input multiplexed ADC which is connected to the PCI bus of the PC.

Visual inspection of VPTs

All of the VPTs received have been inspected visually, to detect obvious defects or anomalies in their photocathodes, anode grids, or other aspects of their appearance. Table 2 summarises the results for those VPTs which were inspected at RAL. The tubes inspected at Brunel do not show significant differences.

In these tables, the photocathode is indicated as “Good” if there is uniform coverage of the whole front face of the VPT; a “Minor flaw” implies a loss of coverage over no more than 20% of the front face, while a “Major flaw” indicates a loss of coverage greater than this. A small proportion of VPTs were found to have a stub of glass protruding beyond the plug of potting compound; this is shown in the table by numbers in brackets. In two cases the VPTs with protruding stubs slightly exceeded the 46mm maximum length laid down in the specification.

There is a clear difference between the two batches. In Batch I, five tubes (of 60) have visible wrinkling in the anode grid, while only one (of 200) in Batch II show this. None of the Batch II VPTs have loose grids, compared with 3 of 60 in Batch I. In Batch I, 60% of the tubes had “Good” photocathodes, while 11.7% displayed “Major” flaws. In Batch II these figures were 71.5% and 6.5% respectively.

Zero-field measurements at Brunel

A total of 100 VPTs was measured in the laboratory, in nominally zero magnetic field, at Brunel. Of these, a batch of fifty and a second batch of twenty were selected at random from those VPTs with bar codes in the range 1--100. A third test batch of thirty tubes was selected at random from VPTs with bar codes in the range 101--260.

Each VPT was measured in a test set-up which permitted the photocathode to be uniformly illuminated with light of mean wavelength 430 nm, produced by hyperbright blue LEDs. The light could be pulsed or steady. With steady illumination, the cathode and anode currents were inferred by measuring the voltages developed across 1 M Ω cathode and anode resistors with digital microvoltmeters. In the case of the anode current, the voltmeter had to be capable of withstanding a common mode DC voltage greater than 1000 V at its input terminals. With pulsed illumination, the anode pulse height was amplified with a low-noise commercial nuclear physics preamplifier and main amplifier, digitised using a fast ADC interfaced to a PC, and the anode pulse height spectrum was evaluated using commercial software. This enabled the mean anode pulse height and the FWHM of the anode pulse height distribution to be evaluated.

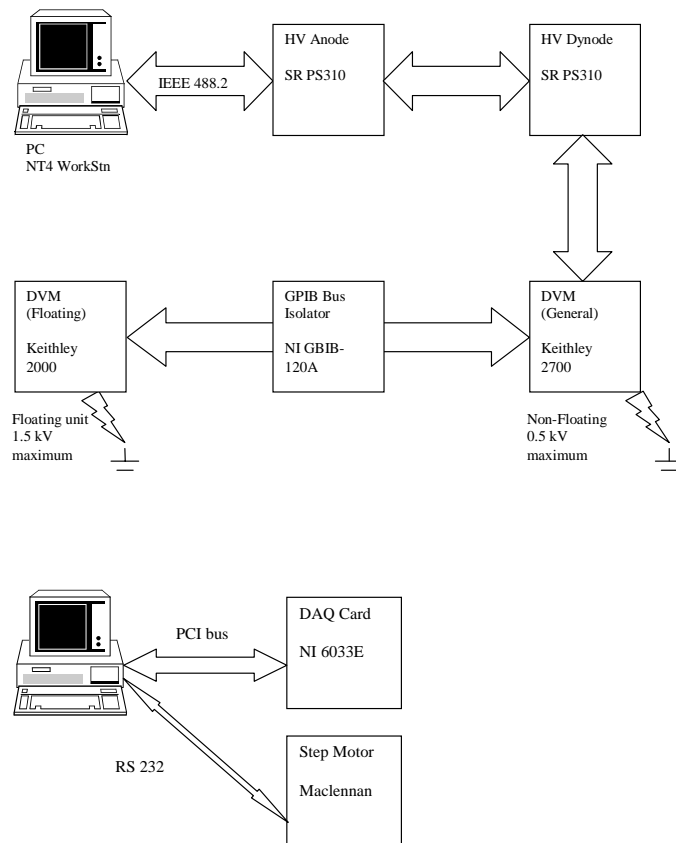


Figure 5. A schematic of the DAQ and control electronics of the 4T test system

The illumination provided by the LEDs was reasonably constant with time. The variation in light output was mainly due to ambient temperature variations, as driving voltages were kept constant to better than 0.1%. The temperature coefficients of the pulsed and DC LEDs were opposite in sign and of the same order of magnitude, such that, given the known variation in the laboratory temperature, both light sources were expected to be stable over the long term to within approximately 3%.

After mounting each VPT in the test set-up, the anode and dynode voltages were quickly ramped up to $V_a = 800\text{ V}$, $V_d = 600\text{ V}$, and the tube left to stabilise for between 3 and 5 minutes. The anode and cathode dark currents were then measured. The DC LEDs were turned on. For a typical VPT, the cathode current with DC LED illumination was about 12nA and the anode current, typically, 110 nA. These values compare with typical dark currents of approximately 50 pA and 600 pA, respectively. The anode and cathode currents were then measured. The dark-current-subtracted cathode current provided a measure of the quantum efficiency of the photocathode, while the ratio of the dark-current-subtracted anode current to the corresponding cathode current provided the current gain of the device. Following the DC measurement, the DC LEDs were turned off and the pulsed LED turned on. The mean anode pulse height and FWHM of the anode pulse height spectrum were measured for approximately 20,000 accepted anode pulses.

Batch I		Photocathode quality		
		Good	Minor flaw	Major flaw
Grid Quality	Good	33	15 (1)	4
	Wrinkled	2	2	0
	Loose	1	0	3

Batch II		Photocathode quality		
		Good	Minor flaw	Major flaw
Grid Quality	Good	142 (7)	44 (1)	13 (1)
	Wrinkled	1 (1)	0	0
	Loose	0	0	0

Table 2. Summary of RAL visual inspection of VPTs. Figures in brackets indicate VPTs where the glass sealing stub projects beyond the potting compound.

Having completed the measurements at 800V/600V, the anode and cathode bias voltages were increased to 1000V/ 800V respectively, the VPT was allowed to stabilise for a few minutes, and the measurements repeated in reverse order; ie a pulse measurement first, followed by a DC measurement and finishing with a measurement of the dark currents at 1000V/800V.

The full measurement sequence on a VPT could normally be completed within 20 to 30 minutes, unless short-term fluctuations in the anode dark current were observed to be greater than ~ 0.5 nA, in which case a longer period was allowed for stabilisation. In a good VPT, any short term dark current fluctuations fall to less than ~ 0.1 nA in a few minutes, although the average dark current may diminish slowly in a time of the order of 24 hours. If the short-term dark current fluctuations failed to show signs of stabilising to below 0.1 nA within about ten minutes, either a reduced-precision measurement of the gain was accepted, (the pulse measurements are much less susceptible to dark current fluctuations), or the gain measurement was abandoned. Figure 6 shows the anode current produced by the DC LEDs plotted against the mean anode pulse height due to the pulsed LED. This correlation provides a powerful, long-term, stability check on the set-up.

The regression line for the third VPT batch, (shown), has a gradient 4.5% lower than that for the first batch. This may be due to the DC LED illumination being slightly different for the two data sets, but could also be due to a difference in the mean ambient temperature. Most of the third batch measurements were made in early January 2001, when the laboratory was warming up from the low-heat Christmas holiday period. The VPT-VPT fluctuations are entirely consistent with ambient temperature fluctuations. On most days the laboratory warmed up by several degrees during the course of the day.

Figure 7, a histogram of the ratio of current gain at 1000V/800V to that at 800V/600V, is another useful consistency check, since for the majority of VPTs the gain ratio is between 1.09 and 1.12.

Figure 8 compares the current gain with the cathode photocurrent, ie the scatter plot effectively compares the secondary emission coefficient of the dynode with the quantum efficiency of the cathode. There is only a small positive correlation. In general, a good photocathode does not guarantee a good dynode and vice versa.

Figure 9 compares the RIE passport values of the current gain with the measurements made at Brunel. There is a strong positive correlation; the outlying points and the slope of 1.1 are not inconsistent with the effect of burn-in, which occurred between the two sets of measurements.

Similarly, Figure 10, which compares RIE QE measurements before burn-in with Brunel post-burn-in values of photocathode current under standard illumination, shows a satisfactory correlation.

Figure 11 is a histogram of the distribution of photocathode current under constant illumination for the first and third batches of VPTs. The first batch has a slightly higher mean, of 12.7 nA, c.f. 12.1 nA for the third batch, a value which is increased by the very high response demonstrated by three of the 30 VPTs in this batch.

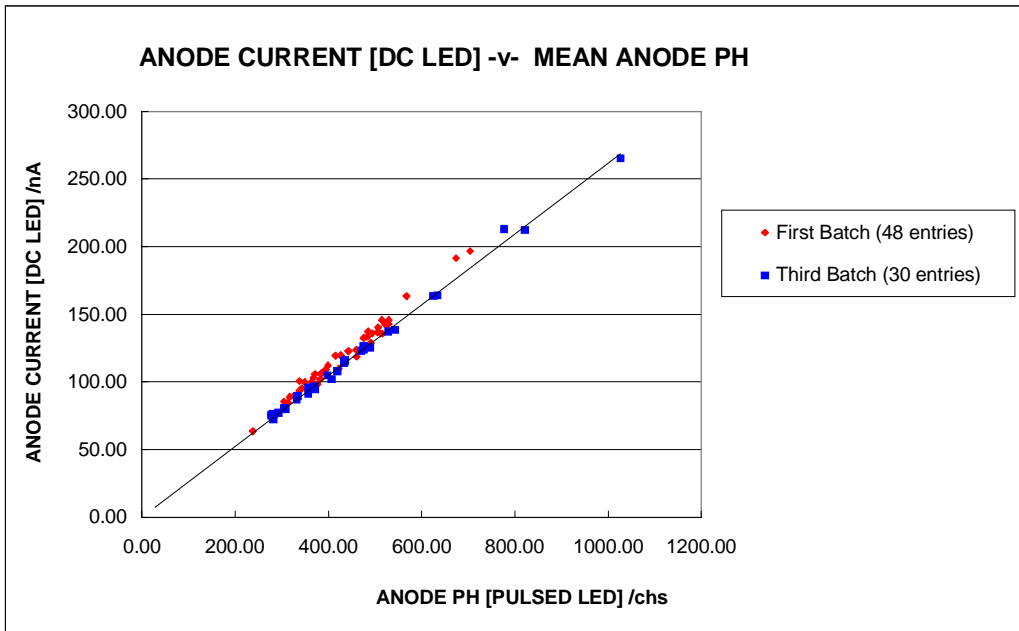


Figure 6. Mean anode current (DC LED) v Mean anode pulse height (Pulsed LED). Measurements on the first batch of VPTs were carried out early in November 2000. Measurements on the third batch were obtained between mid-December 2000, and the end of January 20

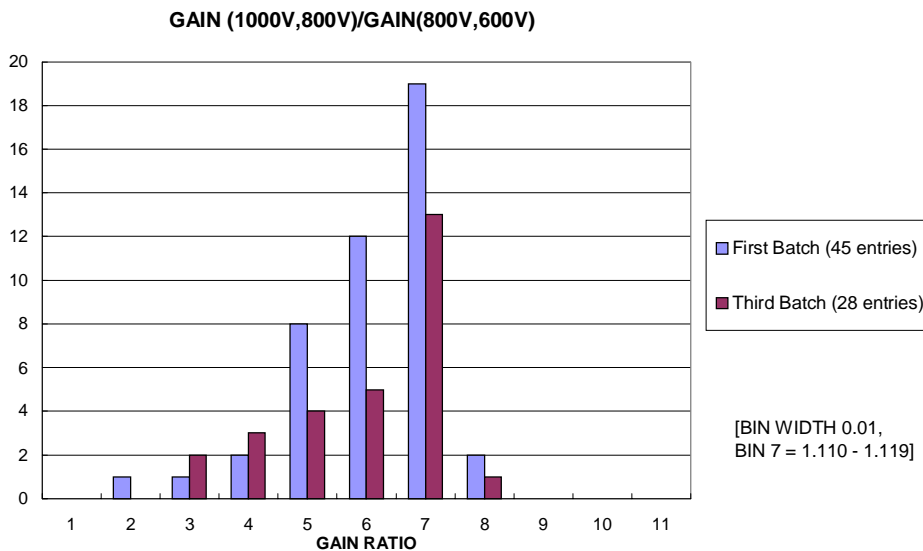


Figure 7. Ratio of the current gain at a bias of $V_a = 1000V$, $V_d = 800V$ to the current gain at a bias of $800V$, $600V$. A number of VPTs, whose dark current fluctuated too rapidly to enable accurate gain measurements to be obtained at both bias voltages, have been excluded from the plot. It is important to note that fluctuating anode dark currents at the nA level appeared not to affect the pulsed LED measurements.

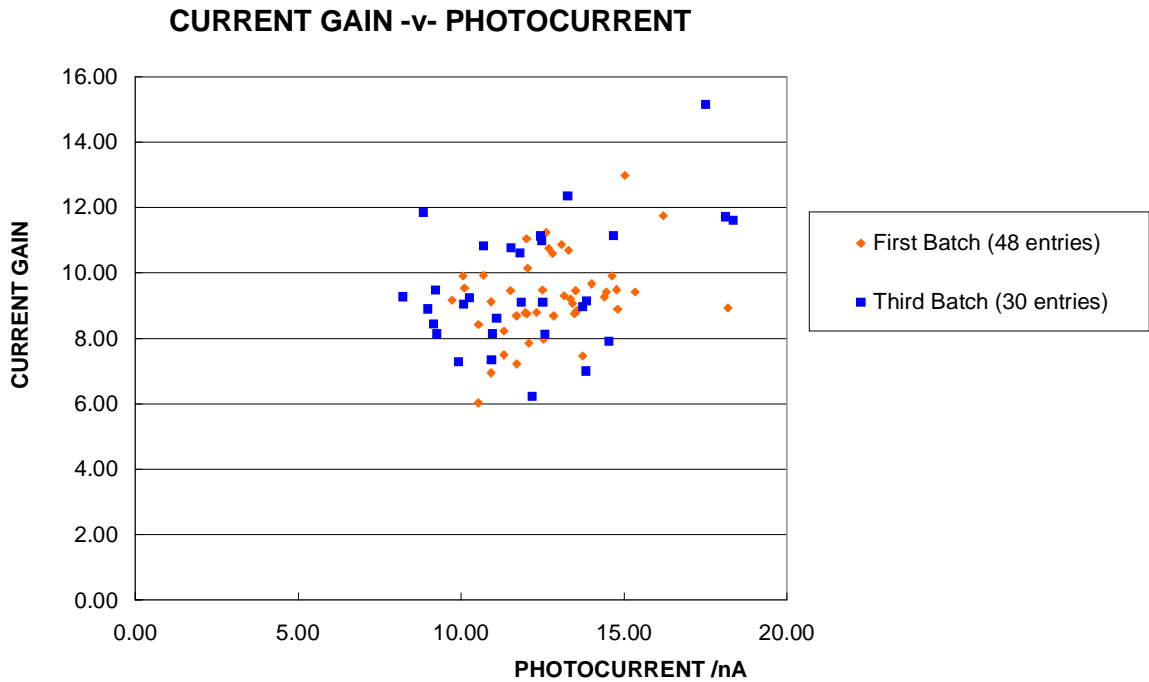


Figure 8. Current gain v photocurrent. There is a very slight positive correlation between current gain and photocurrent, indicating that a good photocathode does not guarantee a good secondary emitting dynode surface and vice-versa.

Figure 12 shows the distribution of anode dark current at 1000V/800V for the third batch. The mean is around 0.6 nA, and only one tube is close to the Technical Specification limit of 2 nA. These currents were measured only a few minutes after the bias voltages were applied and are therefore expected to be upper limits for the dark current. Measurements made after a VPT has been left in the dark with bias on for several hours would, typically, be a factor of two lower. The leakage current measurements for other VPT batches are unreliable because of a small light leak in the set-up, but a similar fraction of VPTs showed abnormally high anode dark currents. These all appear to be associated with abnormally high cathode dark currents. The principal source of high dark current therefore appears to be a very large, but significant, resistance between the cathode and anode. Bearing in mind the construction of the VPT, in which ground potential cathode leads, deposited on the inside of the glass envelope, have to pass the edge of an anode support ring at 1 kV, with a clearance of a fraction of a millimetre, this conclusion appears plausible.

Figure 13 shows the distribution of current gain at 1000V/800V for VPT batches one and three. The mean gain is 9.27 for the first batch and 9.59 for the third. However, excluding the single VPT in the third batch whose gain exceeds 16 reduces the mean gain of the third batch to 9.35, within 1% of the first batch value.

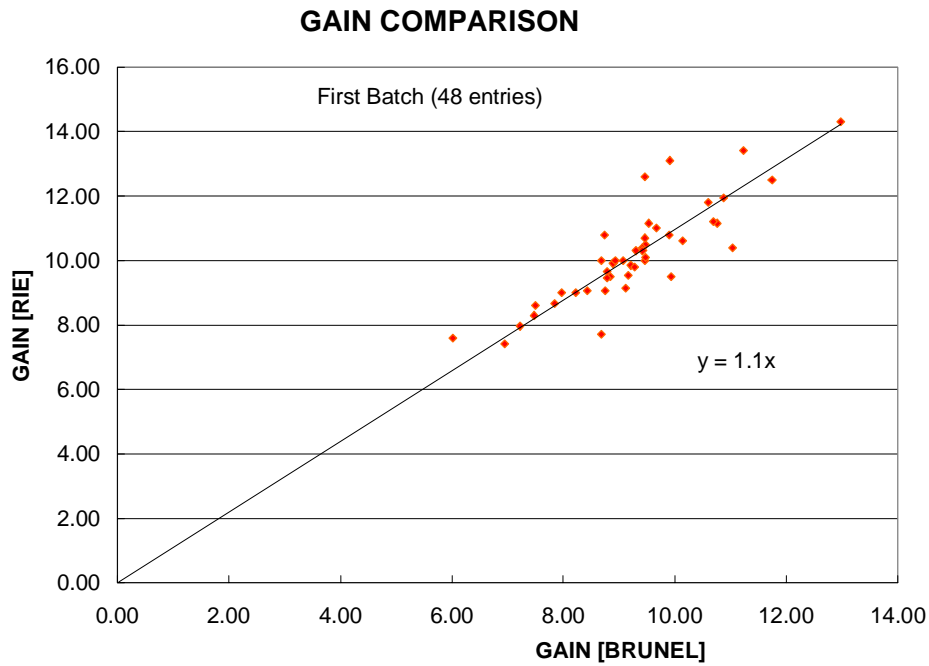


Figure 9. Pre-burn-in gain (RIE) v Post-burn-in gain (Brunel). The correlation is reasonable, and the best fit slope of 1.1 is not incompatible with the expected fall in gain on burn-in.

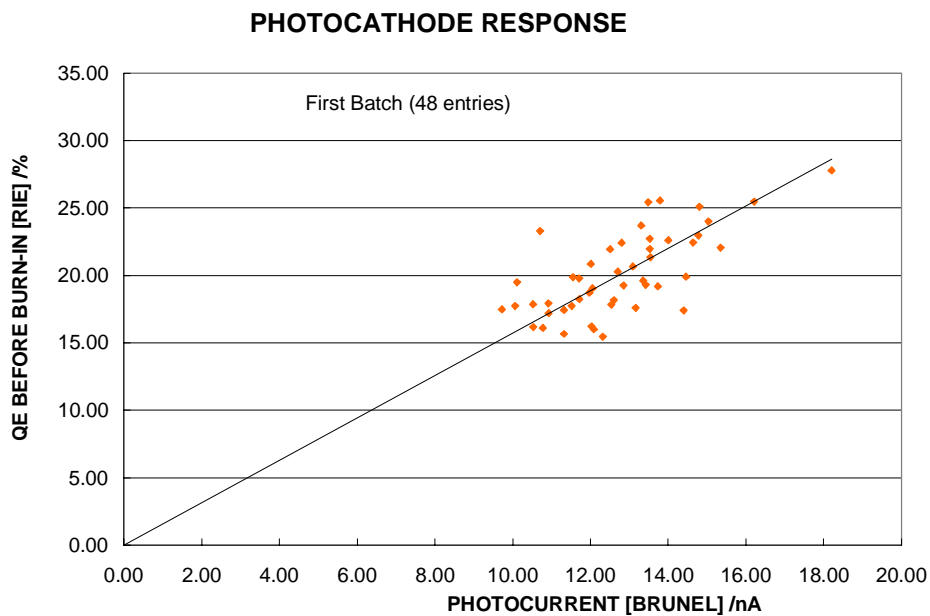


Figure 10. Pre-burn-in photocathode quantum efficiency (RIE) -v- Photocathode response (Brunel). The correlation is reasonable considering the expected effect of burn-in on the photocathode.

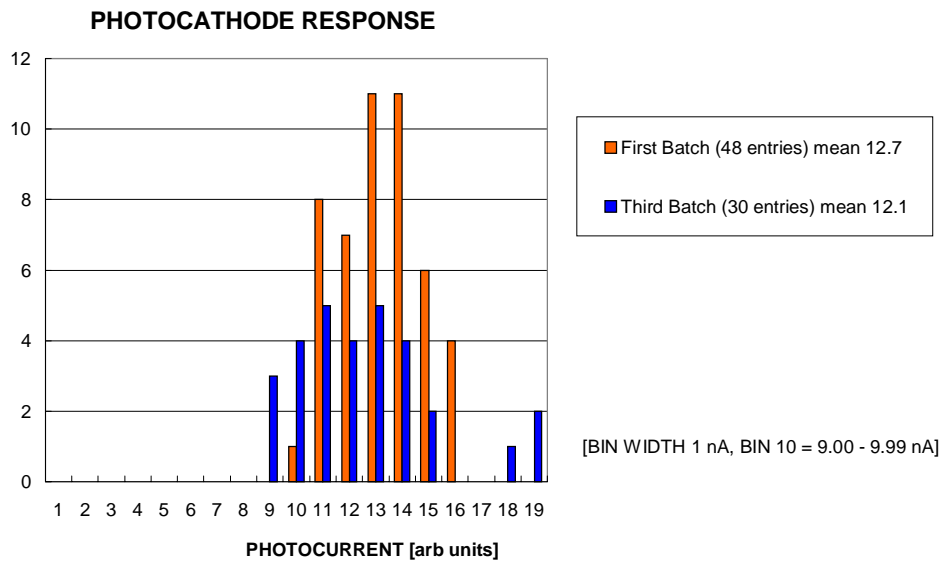


Figure 11. Distribution of photocathode currents for the first and third of the VPT batches. Note the very high photocurrents delivered by three VPTs in the third batch.

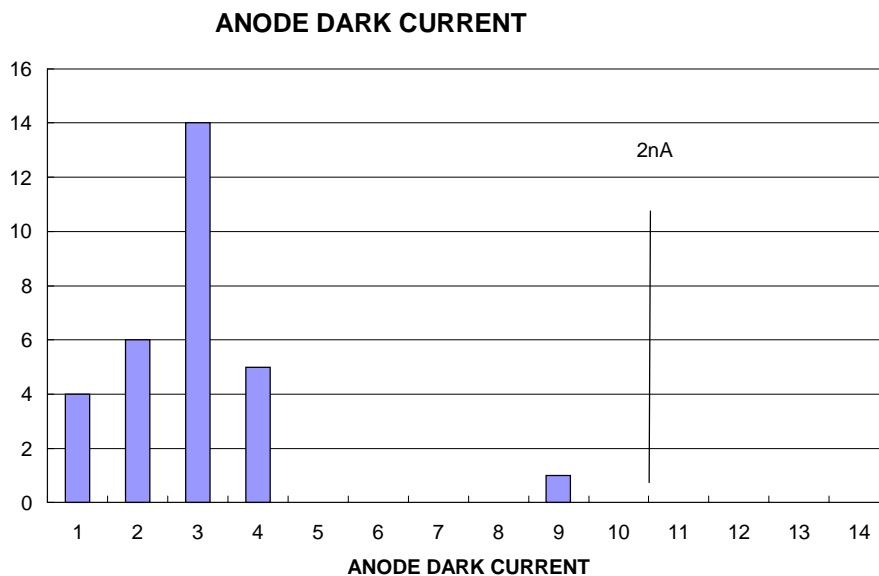


Figure 12. Distribution of anode dark currents (measured approximately three minutes after high voltages applied to the VPT). Most VPTs are well within the Technical Specification limit of 2 nA. Measurements on other batches indicate that VPTs with large anode dark currents appear always to have large cathode dark currents: i.e. when an abnormal anode dark current occurs it indicates anode-cathode rather than anode-dynode breakdown.

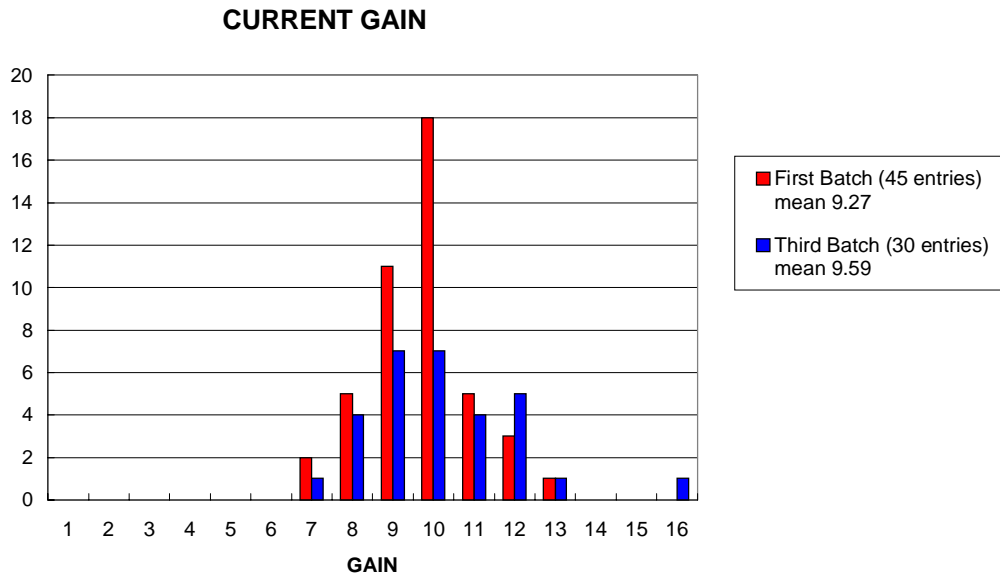


Figure 13. Current gain distribution. One VPT from the third batch has an abnormally large gain

Behaviour of the VPTs in the Brunel test rig at 4T

The ratio of the VPT response at 15° to a 4T field to its response at zero field must be at least 0.75 to meet the technical specification. Figure 14 shows the distribution of this quantity for sample of VPT tubes from Batch I and Batch II.

The repeatability of this critical measurement was determined. Tubes were measured twice, usually after a delay of approximately 12 hours during which they were removed from the torpedo. The repeatability of the measured gain ratio was good. Calculating the distribution of the differences between the first and second measurements on a random sample of 18 Batch I tubes gave a mean of -0.0055 and a sample standard deviation of 0.027.

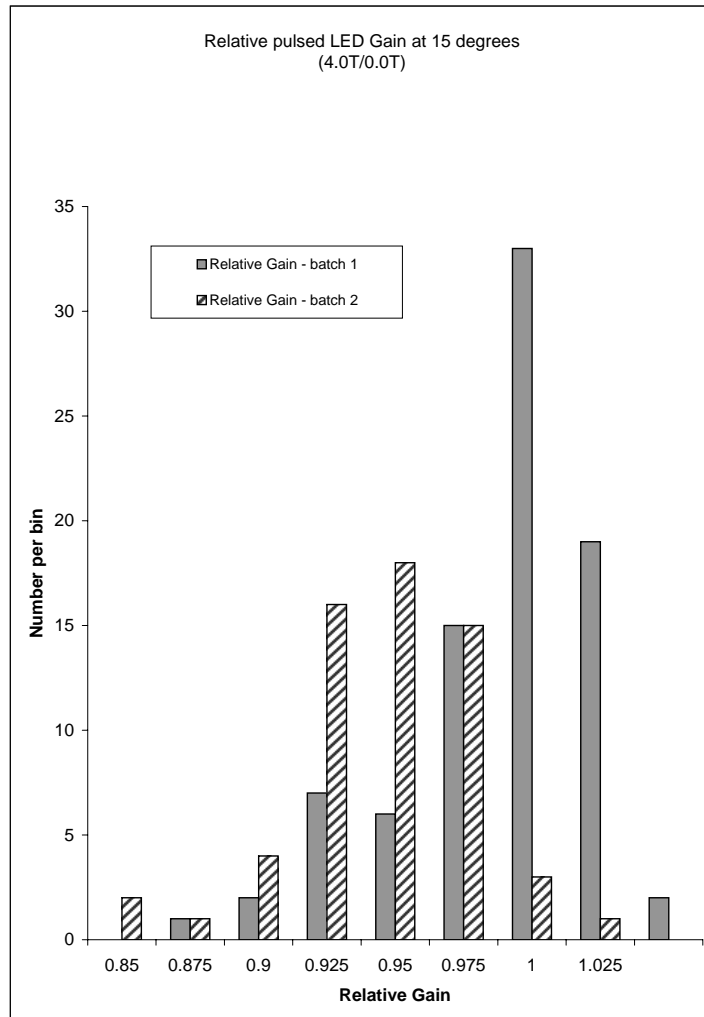


Figure 14. Distribution of $r(4T)/r(0T)$ for all VPTs tested at Brunel.

Measurements in the RAL 1.8T test rig

Magnetic field scans up to 1.8T

The RAL test rig allows VPTs to be operated at any magnetic field up to 1.8T. A standard part of the testing procedure is to scan the field from 1.8T to 0T with the VPT held at an angle of 15° to the field. After each change of field, a short settling period of about 2 minutes is allowed to ensure that the magnet and the VPTs are stable before starting to pulse the LEDs. 1000 LED pulses are measured at each field point. Figure 15 shows the variation in output with field for a typical sample of VPTs.

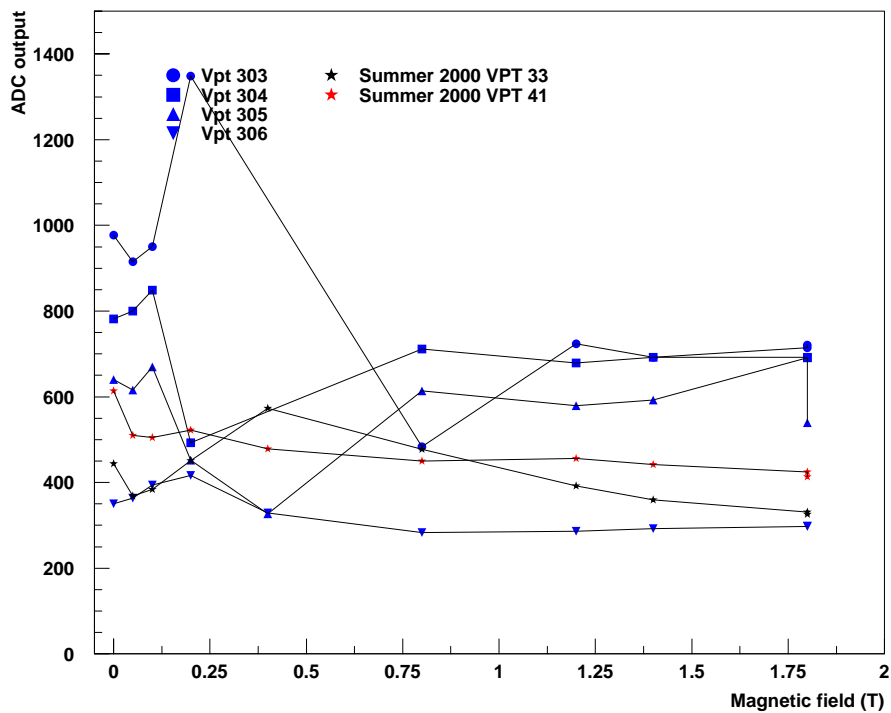


Figure 15. Examples of magnetic field scans on a sample of VPTs.

One of the VPTs in this figure (bar code 303) exhibits a significant instability in the anode pulse size for fields between 0.2T and 0.8T. The pulse width also increases substantially in this range of fields. Approximately 20% of the VPTs display this noisy behaviour at intermediate fields, though in all cases the tubes are stable at fields above 1T.

The ratio of the gain measured at 1.8T to that measured at a nominal field of 0T is shown in Figure 16. The nominal zero-field measurements were taken with the VPTs located between the pole pieces of the magnet, with the magnet current set to 0. The actual field in this configuration is less than 0.01T. The mean of the distribution is 0.86 for VPTs from Batch I, and 0.87 for Batch II. The ratios obtained at 1.8T at RAL are rather lower than those measured at Brunel in the 4T magnet, shown in Figure 14. This is believed to be a consequence of the different illumination of the photocathode in the two test rigs; while the illumination is almost uniform at RAL, in the Brunel rig the centre of the photocathode is more strongly illuminated than the edges, reducing the effect of the magnetic field on the gain.

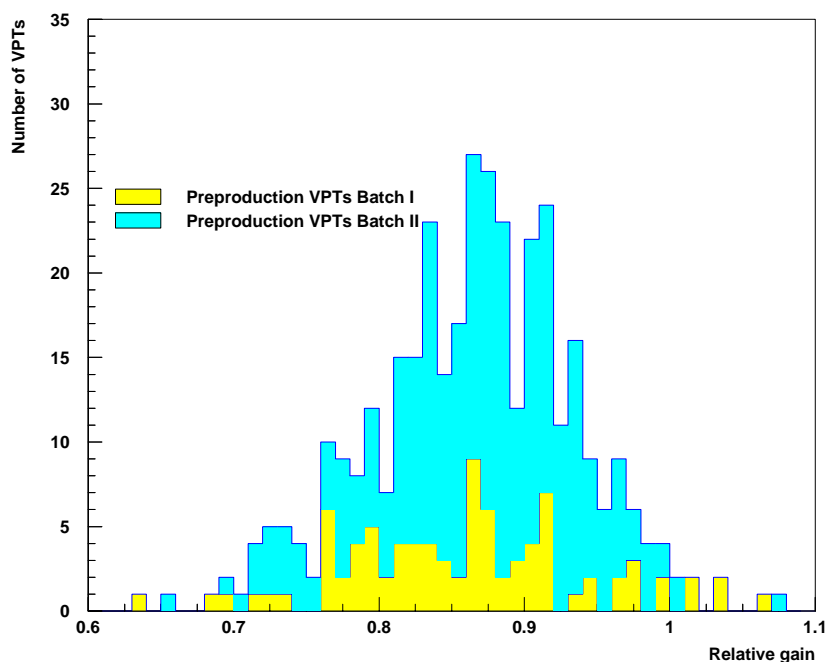


Figure 16. Distribution of $r(1.8T)/r(0T)$ for VPTs tested at RAL.

Angular scans on the VPTs at 1.8T

In the CMS endcap detector, the VPTs will be operated at a range of angles from 7° to 24° to the magnetic field. In the RAL test rig, the devices can be placed at any desired angle with respect to the 1.8T field. In the standard angle scan, measurements are taken at 35 positions from 40° to -40° ; after every movement, a settling period of 30 seconds is allowed so that any induced instabilities in the VPTs can decay before taking data. Again, each measurement consists of 1000 LED pulses. Figure 17 shows the variation in output with angle for a typical sample of VPTs.

The periodicity shown in this figure is seen in all of the VPTs supplied by RIE, and is dependent on the alignment of the anode grid with the axis of rotation. All of the grids have been inspected at RAL using a microscope, and in the standard measurement procedure the grid lines are aligned with the axis of rotation. The two prototype (“Summer 2000”) VPTs shown in the figure were measured in random alignments; the effect of this is to vary the phase of the periodic variation in pulse size.

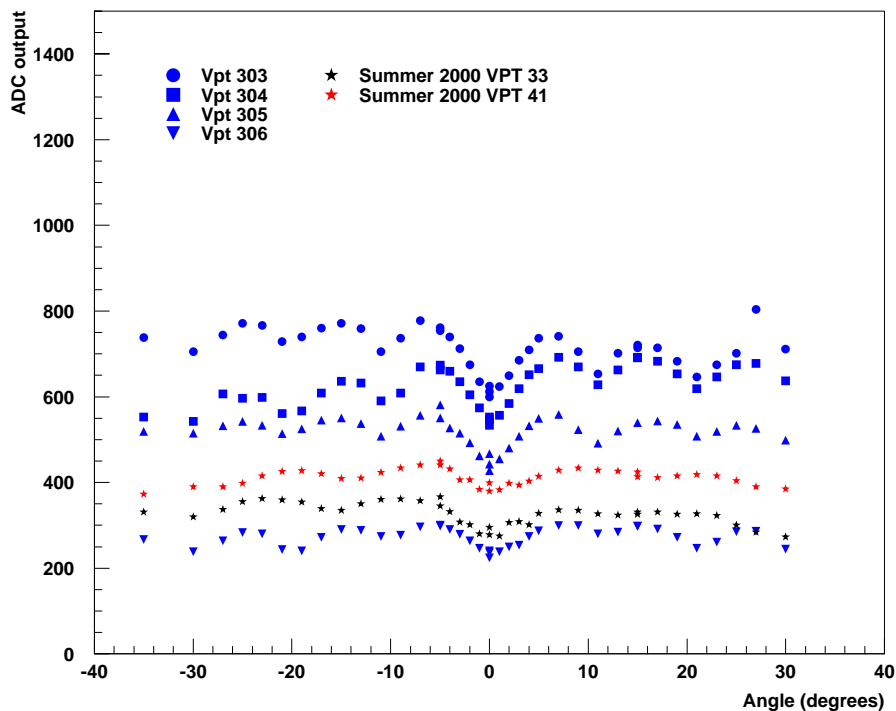


Figure 17. Angular scans at 1.8T on a sample of VPTs.

The specification detailed in [1] requires that the VPT response at 4T in the angular range from 8° to 26° must not vary by more than 10% from the response at 15° . The results obtained in the RAL test rig at 1.8T are indicative of the expected performance at 4T. Figure 18 shows the ratio of the anode pulse heights at 7° and 25° to that at 15° . These angles were chosen to remove the effect of the periodic variation, as they are as the approximate peaks of the response seen in Figure 17. At both angles, most of the VPTs tested lie within the specified range.

Summary of RAL 1.8T measurements

Figure 19 shows the correlation between the anode pulse height measured at 15° to a 1.8T magnetic field and the quality factor Q supplied by the manufacturer. Figure 20 shows the correlation between the VPT output measured at zero field and Q_0 , where $Q_0 = Q/R$ (see Table 1 for the definitions of Q and R).

Figure 21 shows the distribution of anode pulse heights measured in the RAL test rig at 1.8T, with the VPT axis at 15° to the magnetic field. The VPT batches are distinguished by shading. The plot also shows the pulse heights obtained from two prototype VPTs which were gave a satisfactory beam tests at CERN during the summer of 2000.

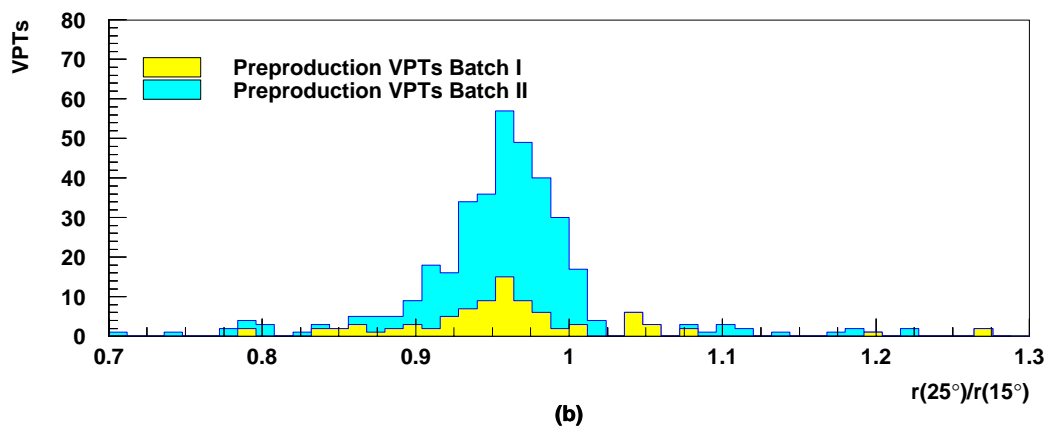
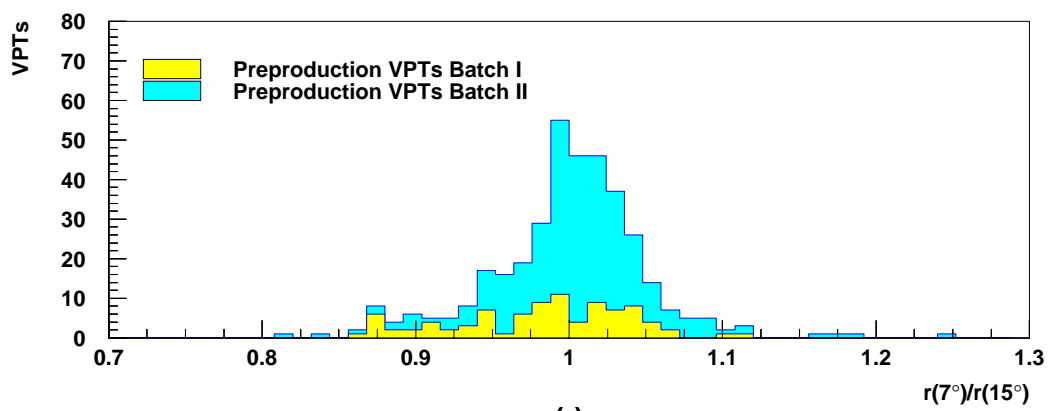


Figure 18. Ratio of the measured anode pulse size at 7° (a) and 25° (b) to that at 15°, in a 1.8T magnetic field.

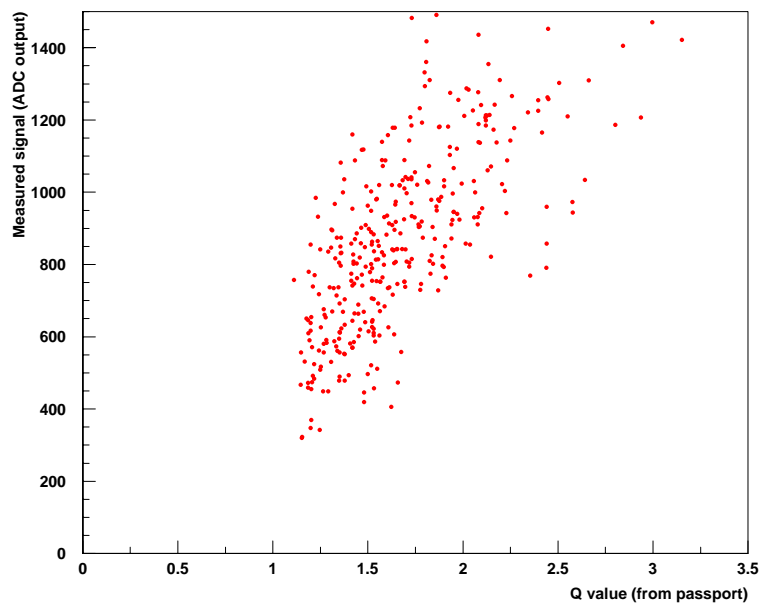


Figure 19. VPT response at 15° and 1.8T v quality factor Q

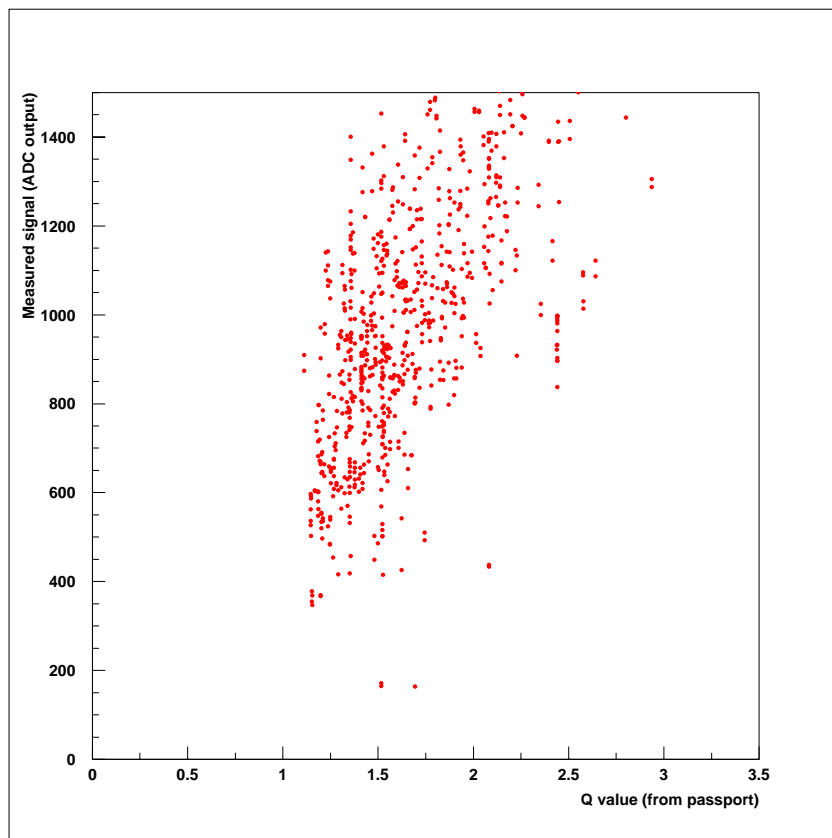


Figure 20. VPT response at zero field v quality factor Q_0

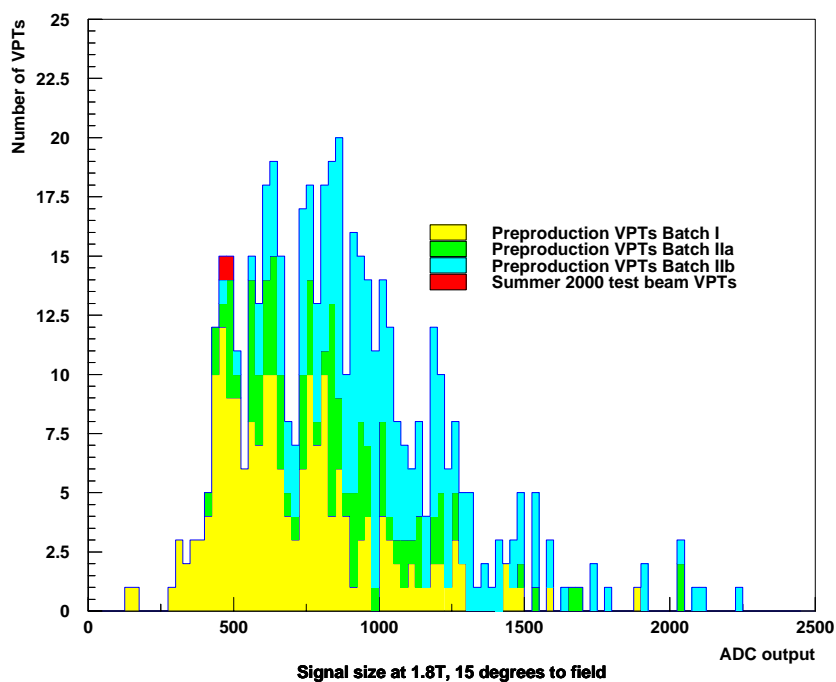


Figure 21. Anode pulse height at 15° and 1.8T.

A parameter of particular significance for the physics performance of the final detector is the ratio of the width of the VPT output to the signal size. Figure 23 shows the distribution of σ/r , where σ is the pedestal-subtracted width of the measured signal distribution, and r is the mean of the distribution, measured at 1.8T and 15°. The two prototype VPTs from Figure 21 are also shown here. The majority of the preproduction VPTs, from both batches, give a lower value of σ/r than the prototypes.

Evolution of VPT parameters

Figure 22 illustrates the behaviour of the VPT performance as a function of the RIE production number recorded on the passport. This number is assumed to be a monotonic function of time. Both the passport Q value and the anode pulse size (measured at 15° and 1.8T) have an upwards trend, presumably reflecting a gradual improvement in production techniques.

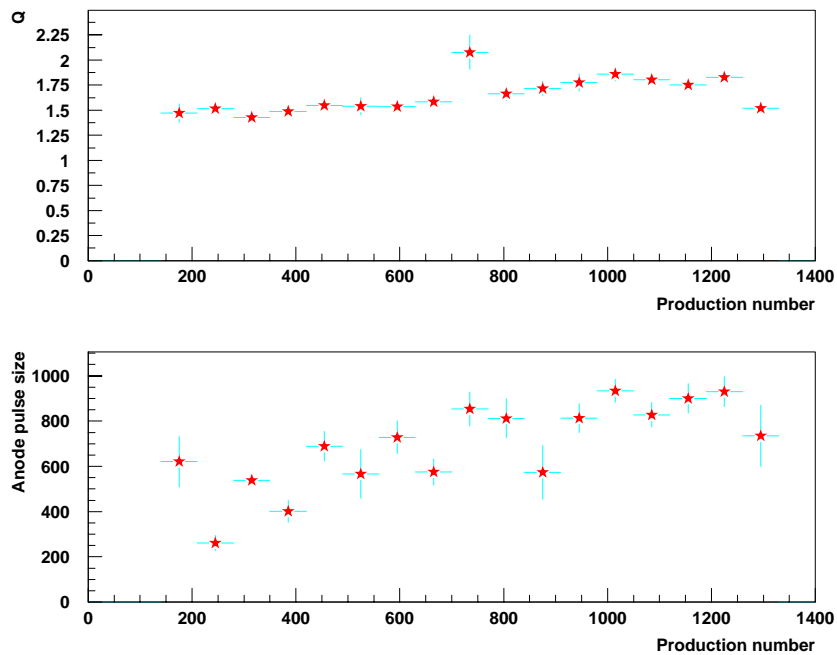


Figure 22. Evolution of Q (from passport) and anode pulse height at 1.8T with RIE production number

Irradiation of VPTs at Brunel

Two of the VPTs from Batch I (bar codes 51 and 63) have been subjected to gamma irradiation using a ^{60}Co source at Brunel., with the anode and dynode maintained at 1000 V and 800 V respectively during the period of irradiation. The anode and cathode currents measured during this procedure are shown in Figure 24. The source was off during the period from 21 to 27 hours. During irradiation, the ratio of anode to cathode current was approximately 10, consistent with the gain of the VPTs. This may be caused by real Cerenkov photons being generated by fast electrons from Compton scattered photons in the tube faceplate, as the tubes were facing the ^{60}Co source. The cathode current data in the first 20 hours of the run were unreliable, and are not shown. There is no significant increase in the anode and cathode currents at the maximum dose so far achieved (2.2kGy).

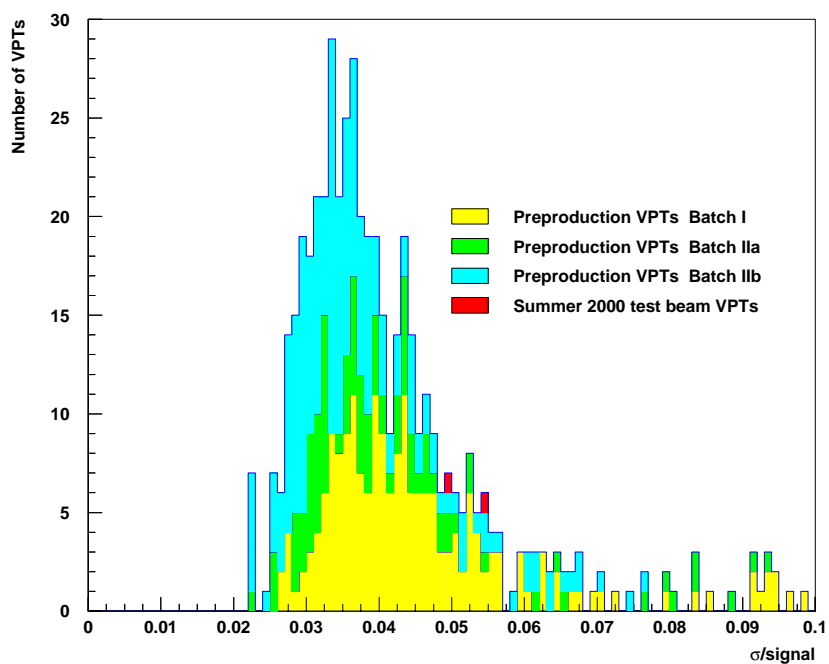


Figure 23. Distribution of σ/r for all VPTs tested at RAL.

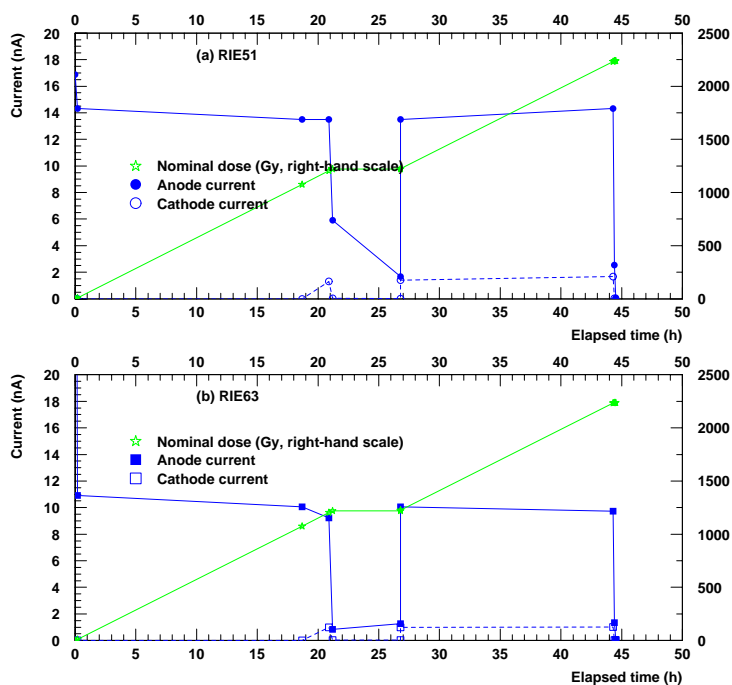


Figure 24. Anode and cathode currents measured during gamma irradiation: (a) RIE51, (b) RIE63.

Summary and Conclusions

The preproduction batch of 500 VPTs supplied by RIE have been subjected to a variety of measurements at RAL and Brunel. The data supplied in the VPT passport is found to correlate well with these measurements. There is a systematic difference of 10% in the gain values measured at RIE and Brunel, but this may be the result of the burn-in procedure. The overall quality factor Q is well-correlated with the measurements in the RAL 1.8T test rig.

Most of the preproduction tubes give a larger anode signal, with a proportionally smaller signal width, than prototype VPTs used in beam tests at CERN in Summer 2000. It is encouraging that the latter devices gave a satisfactory performance in those beam tests.

There is a strong indication that the performance of the VPTs was steadily improved during the manufacture of the preproduction batch.

The large variation in performance, with a factor of approximately 3 between the largest and smallest signal size, is a possible cause of concern, as such variations will limit the dynamic range which can be achieved by the Calorimeter. Since only a small proportion of VPTs lie at the upper extreme of the range, it is proposed to specify an upper limit on Q in addition to a lower limit. This should not reduce the manufacturing yield to an unacceptable degree.

References

[1] 'Technical specification for vacuum phototriodes for the endcap electromagnetic calorimeters of the Compact Muon Solenoid (CMS) experiment', version 5.0, April 27 2000.